



JOURNAL OF POLYMER SCIENCE



Bead-to-Bead Analysis: Introducing an Innovative Methodology for Accelerated Quantitative Analysis of the Welding Behavior of Bead Foams

Marcel Dippold¹ | Alexander Himsel¹ | Justus Kuhnigk¹ | Makrina Chairopoulou² | Maximilian Drexler² | Holger Ruckdäschel¹ ଢ

¹Department of Polymer Engineering, University of Bayreuth, Bayreuth, Germany | ²adidas AG, Herzogenaurach, Germany

Correspondence: Holger Ruckdäschel (holger.ruckdaeschel@uni-bayreuth.de)

Received: 18 September 2024 | Revised: 21 October 2024 | Accepted: 21 October 2024

Funding: This research was funded by the "Bavarian Ministry of Economic Affairs, Regional Development and Energy" within the funding program "Verbundforschungsprogramm Förderlinie Materialien und Werkstoffe," grant number MW-2104-0005.

Keywords: bead foams | EPS | ETPU | welding

ABSTRACT

Performant lightweight components made of bead foams are essential for a sustainable transformation of industry in multiple areas. An in-depth understanding of the welding process is key in reaching maximum mechanical properties. This study presents the novel methodology of Bead-to-Bead analysis, providing a superior way in directly and quantitatively evaluating the welding behavior of bead foams compared with current approaches. Individual beads of expanded polystyrene (EPS) and expanded thermoplastic polyurethane (ETPU) are welded in a rheometer at defined parameters. A subsequent tensile test in combination with the analysis of the welded surface allows the evaluation of shrinkage/softening of the beads during welding and their tensile strength. For EPS, softening of the amorphous material is observed at the beginning of glass transition (~95°C) in addition to an increased welding quality. Residual stresses in ETPU lead to initial shrinkage followed by softening above 140°C. Welding of ETPU starts at 100°C and reaches a maximum at 140°C. The subsequent thermal analysis of the welded beads show the importance of recrystallization processes during cooling due to the formation of new crystalline domains across the bead interfaces. In the absence of such domains, sufficient bonding between beads is not possible.

1 | Introduction

Sustainably management of resources and efficient energy usage are key aspects of our current and future society. To address both of these challenges, lightweight construction by utilizing cellular structures inspired by nature offers solutions for a wide range of industries. Bead foams consist of individual particles which in total form three-dimensional components. Therefore particularly combining both low densities and a high degree of design freedom [1, 2]. Their performance (e.g., physical and mechanical properties) and thus potential applications

depend largely on the quality of the bond between the individual beads [3]. Bead foams are usually processed by the so-called steam-chest molding process, where foamed beads are initially filled into a mold representing the final geometry of the part. Afterwards, hot water steam permeates the cavity heating up the whole beads and especially their surfaces. This increased temperature leads to bead fusion, while retaining a stable foam structure [2]. Interdiffusion of chains at the interface of two beads in contact is causing the fusion process [4–6]. Depending on material characteristics, different fusion mechanisms are present. In the case of amorphous bead foams (e.g., expanded

Marcel Dippold and Alexander Himsel contributed equally to this work

This is an open access article under the terms of the Creative Commons Attribution License, which permits use, distribution and reproduction in any medium, provided the original work is properly cited.

© 2024 The Author(s). Journal of Polymer Science published by Wiley Periodicals LLC.

polystyrene [EPS]), it is assumed that heating above the glass transition temperature T_g increases the mobility of the chains, leading to interdiffusion and physical entanglements across the bead surfaces [3, 7]. For semi-crystalline polymers, like expanded polypropylene (EPP) bead foams a different fusion mechanism is generally accepted. For EPP, bead fusion is feasible due to the double melting peak generated by the controlled production process of the beads. During this foaming process within a stirred autoclave, an isothermal gas saturation phase at elevated temperature (approximately the melting temperature T_m of PP) causes a plasticization effect, which leads to a perfection of the crystals and thus to a higher melting peak $(T_{m \ high})$. The lower melting peak $(T_{m \ low})$ is caused by less perfect crystals, formed during subsequent cooling and foaming. During the fusion process, the steam temperature should be between these two melting peaks to selectively melt only the low melting crystals ($T_{m,low} < T < T_{m,high}$). These molten mobile polymer chains thus contribute to interdiffusion and entanglement processes. The steam temperature must not exceed the higher melting peak $(T_{m,high})$, so that the non-molten higher melting crystals remain intact and the dimensional stability of the foam is maintained. When the molded parts cool down in the cavity, a stable bond is formed between the fused beads based on entangled polymer chains and recrystallized domains across the interface [1, 2, 8–14]. Similar assumptions were also made for the welding mechanism of bead foams made of thermoplastic elastomers like ETPU [15, 16]. These materials show a broad melting range with multiple endothermal peaks due to their structure as block copolymer with crystalline hard and amorphous soft segments [17]. For good adhesion between ETPU beads in the final part, temperatures during welding must be high enough to induce the melting of a sufficient proportion of crystalline hard segments. Throughout the cooling process, polymer chains in those areas can recrystallize within the bead surface and more important, across the interphase [16]. These newly formed crystalline hard segments, in combination with interdiffusion of amorphous areas, bond individual beads and therefore ensure the required transfer of external load.

As the state of the art approach, welding mechanisms of bead foams are primarily investigated by correlating macroscopic mechanical properties of foamed parts produced at varying welding temperatures (steam pressures) with thermal properties of the beads via DSC analysis [2, 15–21]. This approach represents only an indirect analysis of underlying principles. Within this study, the authors introduce a novel methodology for directly testing bead foam welding mechanisms on an efficient lab-scale setup with the possibility of predicting suitable molding parameters. This approach provides a deeper understanding of the intricate process while significantly accelerating the parameter optimization at welding. Thus, the number of trials are reduced contributing to more sustainable research. Understanding the welding behavior as a function of temperature is particularly essential

for steam-less technologies with more inhomogeneous heating like the novel radio-frequency welding [22].

2 | Materials and Methods

2.1 | Materials

In order to evaluate the novel methodology, two commercial bead foam materials with different welding characteristics (amorphous and semi-crystalline) were selected. The properties of both materials can be seen in Table 1.

The sample holders were printed by digital light processing (DLP) on a NXE 400 printer out of xPEEK147-Black (both Nexa3D, Ventura, USA) to fit the universal mounting at the rheometer. In the fully cured state, this material is stable up to 230°C, allowing for usage with most commercial bead materials.

For fixing the individual beads on the sample holders, the two-component epoxy glue PLUS ENDFEST (UHU GmbH & Co KG, Bühl, Germany) was used, cured at 35°C for 1h followed by a minimum of 12h at room temperature. This ensured complete curing and optimal adhesion.

2.2 | Thermal Characterization

Thermal analysis of the materials was performed by modulated differential scanning calorimetry (MDSC) using a Q1000 (TA Instruments Inc., New Castle, USA). This special type of DSC analysis was used to improve signal quality and reduce noise, which can be challenging with foamed samples and especially broad melting peaks as in the case of TPU. The analysis was performed under inert nitrogen atmosphere and with three samples each. Depending on the specific mechanism to be investigated, different variations of MDSC are recommended in literature to improve signal quality. For the investigation of melting areas (ETPU), linear heating rate, amplitude, and period time are specifically set so the actual oscillating temperature never decreases, therefore stated as heat-only [23, 24]. Glass transitions in amorphous polymers like EPS are preferably analyzed under heat-cool conditions, where a temporary reduction in temperature is present. Beads were measured before and after varying welding temperatures in Bead-to-Bead analysis. Parameters for MDSC can be observed in Table 2.

2.3 | Bead-to-Bead Analysis

Inspired by the previous study of Bousmina et al. [25], the authors used a modified test setup on the rotational rheometer MCR 702 TwinDrive (Anton Paar GmbH, Graz, Austria) for development of the novel analysis methodology. In contrast to the

TABLE 1 | Properties of bead foam materials.

Material	Base polymer	Crystalline character	Density (kg m ⁻³)
Infinergy 32-100 U10 (ETPU)	Thermoplastic polyurethane (TPU)	Semi-crystalline	183.17
Styropor F 315 R (EPS)	Polystyrene (PS)	Amorphous	33.08

TABLE 2 | Parameters for MDSC for both materials.

Material	Linear heating rate (K min ⁻¹)	Amplitude (K)	Period time (s)
Infinergy 32-100 U10 (ETPU)	5.0	±0.796	60
Styropor F 315 R (EPS)	10.0	±1.000	30

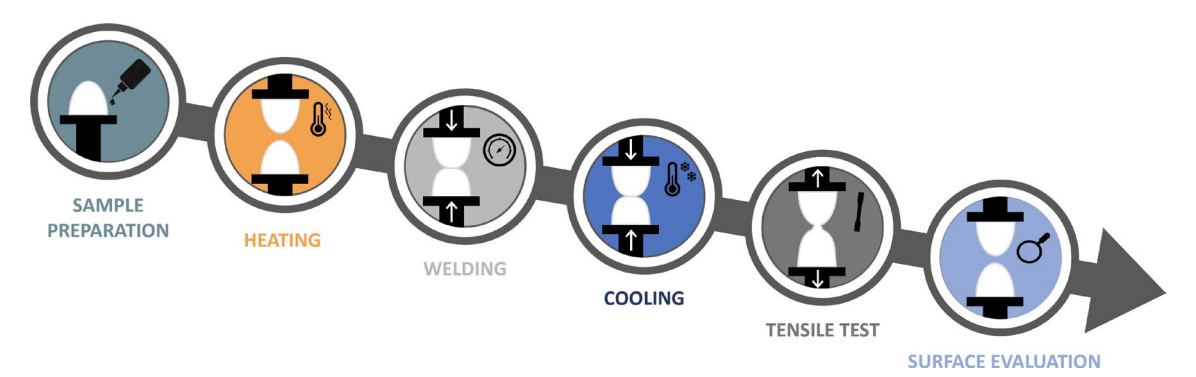


FIGURE 1 | Schematic illustration of the Bead-to-Bead analysis from sample preparation to the evaluation of the contact surface.

study, no rotational motion was used in the setup, due to the deformation of the soft beads and subsequent high degree of error.

As can be seen in Figure 1, sample preparation is necessary as a preliminary step. This setup includes fixing the individual beads onto the specialized printed sample holders. Since perfect central alignment is crucial for representative and repeatable results, notches in perpendicular alignment (visible in Figure 2d) are introduced as visual support during the manual gluing step. Beads with higher diameters, like ETPU, were cut in half prior to this step, while smaller EPS particles could be used as received. The cutting of the ETPU beads was performed in a single stroke using a sharp razor blade. Thereby, the elastic beads were subject to minimal deformation and retained their original shape without damaging their internal structure.

The samples are placed inside the rheometer by universal fixations and manually aligned in rotation with a minimum distance in between without contact (Figure 2a). This ensures that the beads, especially their surface, heat up fast and homogeneously. Samples are then heated to the desired measurement temperature including a stabilization time of 60s to take into account the isolation properties of foams. Depending on the targeted temperature, this step usually only takes a few minutes.

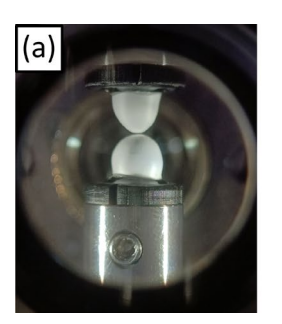
For the actual welding step at isothermal conditions, the bead surfaces are brought into direct contact by using the upper horizontal drive of the device until a defined contact force is reached. Depending on bead type, density, and size, this force has to be adjusted to mimic compressions close to the actual welding process. For this study, the contact force was set constant to 0.50 and 0.25 N for EPU and EPS respectively. This procedure ensures sufficient contact area without over-compressing the samples at all investigated temperatures (Figure 2b). Besides welding temperature and contact force, the welding time can be adjusted independently as the third crucial parameter. In accordance with the industrial process and mitigation of run-in effects, a constant welding time of 5 min was selected for all trials [16, 20]. Typical temperature

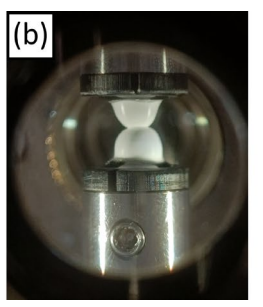
and force curves along the complete cycle from welding and subsequent steps are schematically shown in Figure 3.

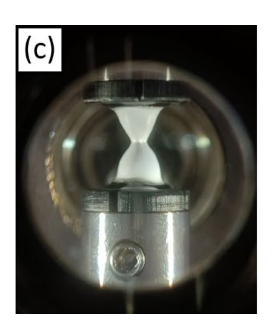
As indicated by the drop in temperature after welding in Figure 3, a subsequent cooling step is added to reach a standard testing temperature of 23°C followed by a 5min stabilization time to guarantee homogeneous conditions throughout the bead volume. Further interdiffusion after the welding step must be minimized to observe reproducibly results. For this purpose, liquid nitrogen is used to rapidly cool down samples after welding. Down to around 30°C, cooling rates of approximately 15–20 K min⁻¹ are achieved, depending on the initial temperature. The slight interruption in cooling around 30°C is based on an internal switch in cooling method within the rheometer from the liquid nitrogen to the standard intercooler. Recrystallization plays a key role in the adhesion of semicrystalline materials like ETPU [16]. Due to its high dependency on the cooling rate, comparable cooling times to, for example, steam chest molding in the range of several minutes could be achieved. During this step, the contact force is kept constant.

The last phase within the rheometer as a continuous process is the modified tensile test at 23°C. Due to limitations in the rheometer and to take varying bead sizes into account, a reduced strain rate of 0.5 mm min⁻¹ was set, compared with standardized 500 mm min⁻¹ (DIN EN ISO 1798:2008-04). As can be seen in Figure 3, this initially reduced previous compression between the beads until tension is present. This leads to an elongation of the beads with increasing stress within the newly formed interface between the two beads (Figure 2c). Following the nearly linear elastic curve, maximum strength of the interface is reached, leading to partial and subsequent complete debonding of the two beads or rupture within one of the beads.

To ensure a comparison between varying bead sizes, the contact area between the two beads is analyzed in a microscope by the clearly visible indents on the beads surfaces and calculated on the basis of an elliptical shape (Figure 2d). The average of both







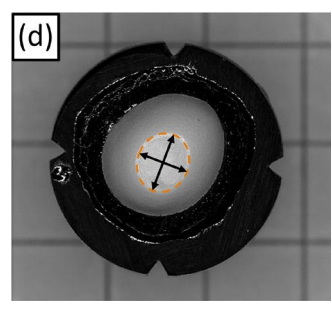


FIGURE 2 | Pictures inside the rheometer during heating (a), welding (b), tensile test (c), and the evaluation of the welded surface (d) of ETPU afterwards.

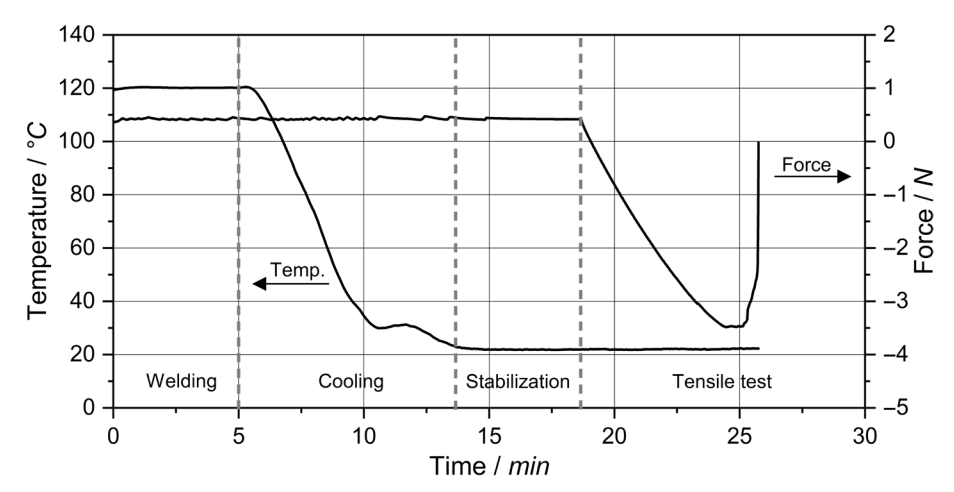


FIGURE 3 | Temperature (left) and force applied on the beads (right) over the continuous section of the Bead-to-Bead procedure inside the rheometer.

sides is used for transforming the force into more uniform stress values. In the case of intra-bead failure, the actual welding surface cannot clearly be identified, so the area of rupture is used instead. A minimum of three samples was tested at each parameter for statistical relevance.

In general, this methodology enables an efficient and direct analysis of the welding quality in dependence of the most relevant parameters for interdiffusion between polymer surfaces including time, temperature, and pressure [5, 26]. By process adjustments, these parameters can be studied nearly separately. For the factor time, as seen in Figure 3, the beads are additionally affected by elevated temperatures in the beginning of the cooling step where further interdiffusion processes may occur. At these elevated temperatures, slight changes in volume of the beads by shrinkage or softening occurs. This can lead to a slight de- or increase of contact pressure between the surfaces, which is considered to be neglectable for the low values encountered in the actual welding process.

The first results of this novel methodology for EPS and ETPU are shown and discussed in the subsequent sections.

3 | Results and Discussion

Volumetric changes during welding of beads can significantly influence the properties of the molded part. Heating of thermoplastic bead foams can induce different phenomena resulting in

expansion or shrinkage [2, 19, 21]. At the elevated welding temperatures, shrinkage is the major effect, which can be divided into two types; softening and relaxation. This shrinkage can significantly reduce contact pressure between the beads and, in the worst case, result in gaps between the beads preventing any welding. During molding, this phenomena can be mitigated to a certain extent by pre-pressurization of the beads, post expansion by residual blowing agent, or compression after filling.

The amorphous character of EPS causes increased softening of the polymer during heating, based on enhanced chain mobility especially above the glass transition. In regard to the Bead-to-Bead analysis performed at constant contact force, this softening leads to an increase in the contact area between the increasingly compressed beads. As can be seen in Figure 4, the contact area only increases slightly up to 90°C, before an upward step is observed at 95°C, correlating with the onset of glass transition at 97.0 ± 0.4 °C (Figure 6).

With further increase in temperature, contact area shows a constant increase with one slight deviation at 105°C, which could be caused by misalignment of the beads during the gluing step or fluctuations in bead geometry. This softening induced increase in contact area of EPS at higher temperatures is also visible in Figure 5.

At welding temperatures above 100°C, the first failure inside the EPS beads occurs, leading to challenges in a precise analysis of the contact area.

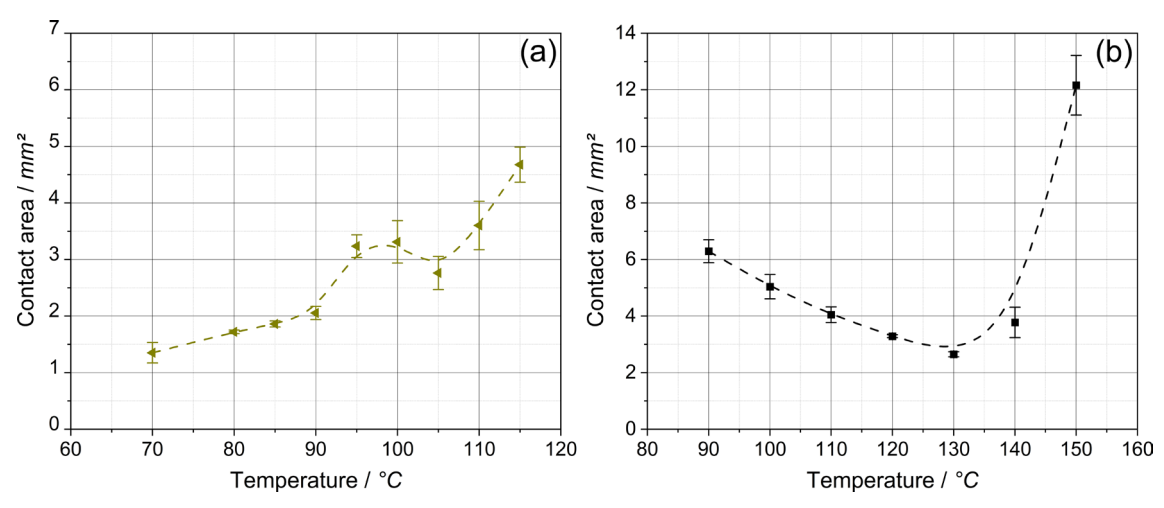
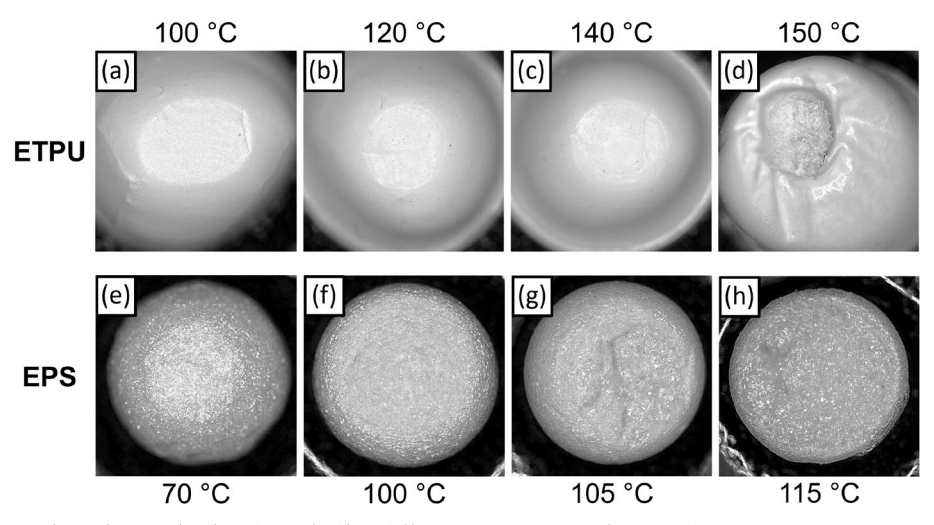


FIGURE 4 | Contact area between the beads for EPS (left) and ETPU (right) measured after the tensile test over the welding temperature.



 $\textbf{FIGURE 5} \quad | \quad \text{Welding surface of ETPU (a-d) and EPS (e-h) at different temperatures after tensile test.}$

On the other hand, a different behavior is observed for ETPU (Figure 4). Up to a welding temperature of 130°C, the contact area declines from more than 6 mm² to less than 3 mm². In contrast to EPS, the cell walls inside the beads contain significant residual stresses, caused by the foaming process. Based on the fine cellular morphology, it is assumed that the ETPU beads used in this study are produced by autoclave foaming. This induces high elongation during expansion followed by a fast cooling. Polymer chains are frozen in a stretched state, which leads to relaxation at elevated temperatures. This relaxation induces a three-dimensional shrinkage, which is almost independent of external compression. In Figure 5, the shrinkage of the ETPU bead is visible at the tip, while being unable to deform at the bottom due to the fixation by the glue. Above 130°C, a significant proportion of hard segments is molten, thus weakening the structural integrity of the cellular structure. This softening of the material results in a steep increase in contact area between the beads during the analysis. Similar to EPS, the intracellular structure of the beads acts as weakest link, leading to a fracture within the beads. Precise analysis of the actual contact area is challenging.

Besides the evaluation of bead shrinkage, the direct measurement of welding quality is the main focus of this novel methodology. For EPS, tensile strength increases slightly up to 95°C and more rapidly at temperatures above (Figure 6c). Above 105°C, tensile strength reaches a maximum and subsequently decreases slightly, likely caused by severe deformation and damage of the beads. Comparing these results with the fracture surface in Figure 5, it can be concluded that above 105°C any theoretically improved welding quality is not measurable, as the foam structure of the beads acts as weakest link. At this point, the maximum mechanical property of a part would be reached. As described earlier, this increase in welding quality corresponds directly to the temperature range of glass transition of the neat bead, which can be seen in Figure 6a as hatched area. Thermal analysis of the beads after being tested in Bead-to-Bead analysis at 80°C, 100°C, and 110°C show no changes in glass transition. Since EPS is usually processed in steam chest molding at absolute saturated steam pressures of around 1.0-1.5 bar (100°C-110°C), this clearly demonstrates the good transferability of the methodology to the industrial welding process and its predictive capabilities [1].

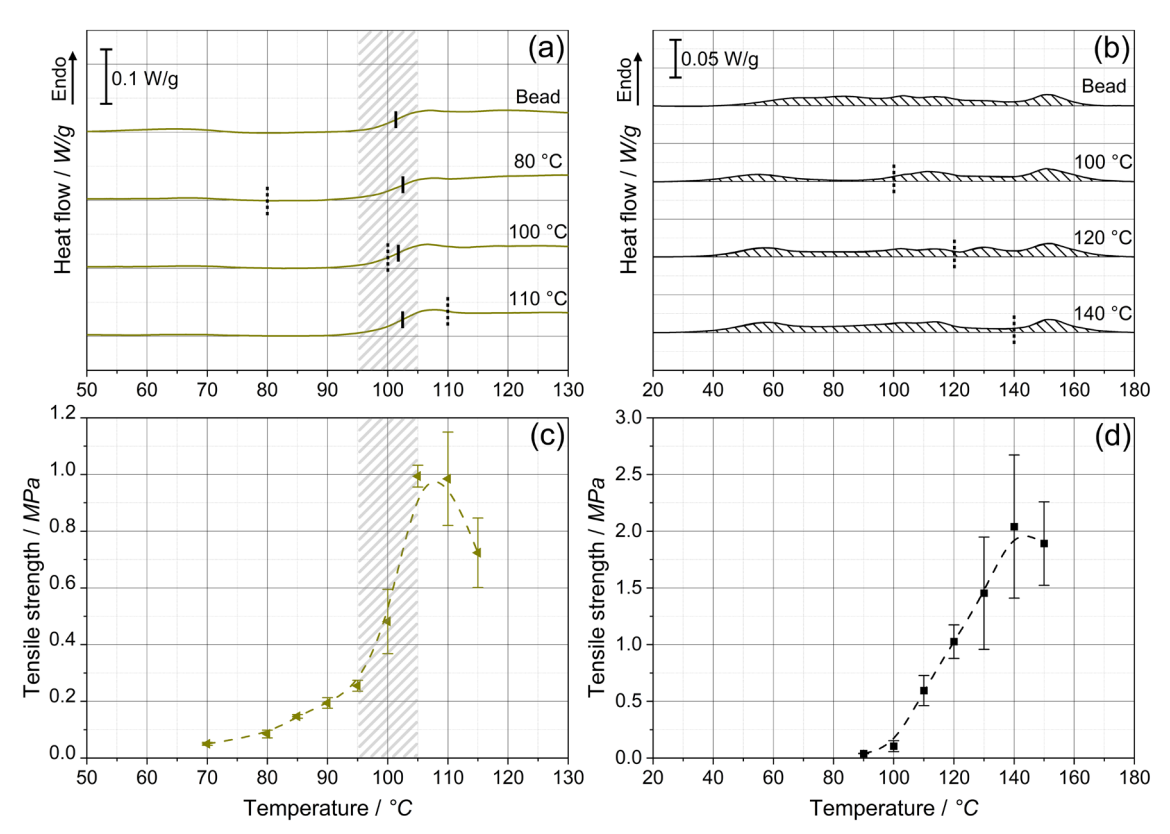


FIGURE 6 | DSC first heating curves of EPS (left) and ETPU (right) beads virgin and after analysis at varying temperatures (a, b). Tensile strength obtained from Bead-to-Bead of both materials as a function of welding temperature (c, d). The hatched area for EPS should act as visual guidance for the glass transition range, while the vertical solid lines represent the glass transition temperature. The dotted vertical lines in (a, b) indicate the welding temperature in Bead-to-Bead prior to DSC analysis.

Similar to EPS, the DSC analysis and tensile strength of ETPU is shown in Figure 6b,d, respectively. Based on its semicrystalline character, partial melting of the bead surface is crucial for the welding process. The melting area can be observed in a typical wide range with multiple smaller endothermal peaks for the virgin bead. By overlapping the tensile strength curve with melting range, a clear temperature shift is visible. First adhesion between the beads starts at temperatures within the melting range. Subsequently, an almost linear increase in welding quality is observed from 90°C to 140°C, before reaching a limit. At this point, adhesion is so strong that the bead itself acts as the weakest part in the system resulting in intra-bead failure (visible in Figure 5d). In order to understand this behavior, a closer look at the DSC curves of the beads after testing is needed. At a welding temperature of 100°C, a more pronounced peak is formed at around 110°C. This indicates the partial perfection of crystalline regions induced by the annealing process, which is schematically shown in Figure 7 and already reported in literature for other thermoplastic elastomers [17].

Higher melting crystals above that temperature remain unchanged. Since welding of ETPU is highly dependent on newly formed crystalline domains across the bead interfaces, recrystallization after the welding step is essential. At a welding temperature of 100°C, only a small endothermal peak is formed at around 55°C during the cooling process after welding. Therefore almost no recrystallized regions are present to bridge the gap between the beads, resulting in low tensile strength [16]. If the welding

temperature is increased to 120°C, a similar peak is observed slightly above that temperature indicating partial perfection of crystalline domains. The high temperature melting peak again is not influenced. Unlike before, at this welding temperature significant recrystallization during cooling is visible, resulting in an increased tensile strength (Figure 7). At an even higher welding temperature of 140°C, this effect is even more pronounced. Any peak formed by crystalline perfection is assumed to shift into the high temperature melting peak and is therefore not clearly visible. By comparing the observations of shrinkage of ETPU in Figure 4b with the melting range from DSC analysis, it can be concluded that the high temperature melting peak from 140°C to 160°C is essential for the structural integrity of the bead. Thus, if welding temperatures are set above 140°C, the cellular structure is at risk of being damaged, which can deteriorate the mechanical performance of any final part and should therefore be avoided.

In summary, the absolute values for tensile strength are within the same order of magnitude observed for samples from steam chest molding for both materials [1, 15, 16, 19, 27, 28]. For a fair comparison between the Bead-to-Bead analysis and the real welding process, two aspects must be considered. (i) By applying a constant contact force during welding and cooling, the shrinkage of the beads can be analyzed. However, in real welding processes the beads experience only an initial compression during the filling of the mold. Subsequent shrinkage or softening of the material will therefore reduce the contact force or can even lead to the formation of gaps between the individual beads. Due to the high flexibility of the rheometer setup, switching from constant

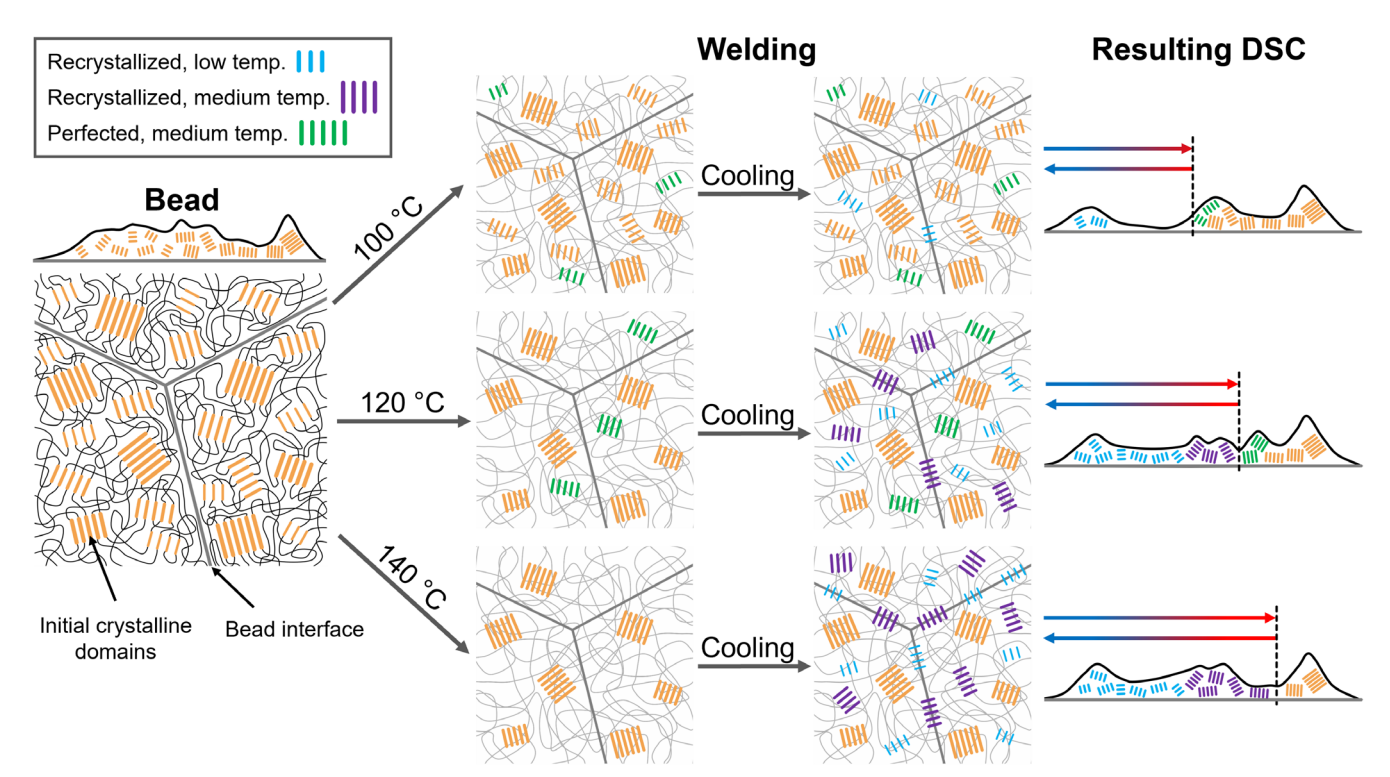


FIGURE 7 | Schematic illustration of the changes in crystalline domains of ETPU at the bead interface during welding and subsequent cooling. This leads to partial perfection of crystals (dark green) and thermodynamically driven recrystallization (blue and purple) within the polymer and across the interface during the cooling process.

force to constant compression during welding is possible, which is in focus for future studies. (ii) Second, the contact area is essential for the calculation of the tensile strength in Bead-to-Bead analysis. Besides the challenges in precise measurement at high temperatures or rupture of beads, a real molded part forms a three-dimensional network of beads not only in the direction of an external force. Transmission of load is also distributed over the whole bead surface. Therefore, reduced interfacial adhesion is necessary to exceed the strength limit of the foam structure, limiting the overall tensile strength of the part.

4 | Conclusion

In this study, a novel analysis methodology for the direct measurement of welding quality of various bead foams is presented. By precise sample preparation and the usage of 3D printed holders, beads can be welded at defined temperature, contact force, and time. In situ tensile testing in the end of the welding process, combined with the evaluation of contact area, allows the analysis of bonding as tensile strength. Analyzing the contact area, deformation of the beads during the welding process can be observed. For EPS, the softening of the base polymer with increasing temperature is visible with a pronounced step at the beginning of the glass transition. In comparison, ETPU experiences an initial shrinkage due to residual stresses inside the cell walls originating from the bead manufacturing process. Once the high melting peak of the materials is reached, softening effects dominate, which indicates its relevance for structural stability. In Bead-to-Bead analysis, the state of the art welding theory of EPS was quantitatively confirmed. An increase around glass transition based on enhanced chain mobility is shown, which is also in line with parameters from real molding processes. On the other hand, analysis of ETPU provides a deeper insight into the intricate welding behavior. For this semi-crystalline material, the promotion of adhesion between the beads by newly formed crystalline domains at the interface was validated. Welding temperatures within the broad melting range are necessary to initiate interfacial diffusion and recrystallization during the subsequent cooling process. As known for bead foam parts, at a certain point the mechanical properties are limited by internal failure of the cellular structure, which was also observed in this analysis at higher welding temperatures.

In contrast to the current approach by an indirect evaluation of the welding behavior of bead foams via DSC analysis, Bead-to-Bead analysis outperforms existing techniques by a more detailed and direct investigation of important phenomena. This new approach will significantly improve understanding of bead foam welding mechanisms and therefore accelerate further developments in the area of lightweight parts. Based on results shown, the methodology is independent of bead type and suitable for other welding technologies besides steam chest molding like radio-frequency welding. For future studies, these results can be implemented into multiphysical simulation for a direct and local prediction of mechanical properties in complex bead foam parts.

Acknowledgments

The authors would like to acknowledge the Bavarian Polymer Institute (BPI) for providing access to different analysis methods.

Conflicts of Interest

The authors declare no conflicts of interest.

Data Availability Statement

The data that support the findings of this study are available from the corresponding author upon reasonable request.

References

- 1. J. Kuhnigk, T. Standau, D. Dörr, C. Brütting, V. Altstädt, and H. Ruckdäschel, "Progress in the Development of Bead Foams—A Review," *Journal of Cellular Plastics* 58, no. 4 (2022): 707–735.
- 2. D. Raps, N. Hossieny, C. B. Park, and V. Altstädt, "Past and Present Developments in Polymer Bead Foams and Bead Foaming Technology," *Polymer (Guildf)* 56 (2015): 5–19.
- 3. J. Rossacci and S. Shivkumar, "Influence of EPS Bead Fusion on Pattern Degradation and Casting Formation in the Lost Foam Process," *Journal of Materials Science* 38, no. 11 (2003): 2321–2330.
- 4. R. P. Wool, B.-L. Yuan, and O. J. McGarel, "Welding of Polymer Interfaces," *Polymer Engineering and Science* 29, no. 19 (1989): 1340–1367.
- 5. Y. H. Kim and R. P. Wool, "A Theory of Healing at a Polymer-Polymer Interface," *Macromolecules* 16, no. 7 (1983): 1115–1120.
- 6. H. Qiu and M. Bousmina, "Determination of Mutual Diffusion Coefficients at Nonsymmetric Polymer/Polymer Interfaces From Rheometry," *Macromolecules* 33, no. 17 (2000): 6588–6594.
- 7. J. Rossacci and S. Shivkumar, "Bead Fusion in Polystyrene Foams," *Journal of Materials Science* 38, no. 2 (2003): 201–206.
- 8. M. Nofar, Y. Guo, and C. B. Park, "Double Crystal Melting Peak Generation for Expanded Polypropylene Bead Foam Manufacturing," *Industrial and Engineering Chemistry Research* 52, no. 6 (2013): 2297–2303.
- 9. M. Nofar, A. Ameli, and C. B. Park, "Development of Polylactide Bead Foams With Double Crystal Melting Peaks," *Polymer (Guildf)* 69, no. 1 (2015): 83–94.
- 10. D. Klempner and K. Frisch, *Handbook of Polymeric Foams and Foam Technology* (München: Hanser, 2004).
- 11. S. Nakai, K. Taki, I. Tsujimura, and M. Ohshima, "Numerical Simulation of a Polypropylene Foam Bead Expansion Process," *Polymer Engineering and Science* 48, no. 1 (2008): 107–115.
- 12. W. Zhai, Y. W. Kim, and C. B. Park, "Steam-Chest Molding of Expanded Polypropylene Foams. 1. DSC Simulation of Bead Foam Processing," *Industrial and Engineering Chemistry Research* 49, no. 20 (2010): 9822–9829.
- 13. W. Zhai, Y. W. Kim, D. W. Jung, and C. B. Park, "Steam-Chest Molding of Expanded Polypropylene Foams. 2. Mechanism of Interbead Bonding," *Industrial and Engineering Chemistry Research* 50, no. 9 (2011): 5523–5531.
- 14. N. Hossieny, A. Ameli, and C. B. Park, "Characterization of Expanded Polypropylene Bead Foams With Modified Steam-Chest Molding," *Industrial and Engineering Chemistry Research* 52, no. 24 (2013): 8236–8247.
- 15. C. Ge, Q. Ren, S. Wang, W. Zheng, W. Zhai, and C. B. Park, "Steam-Chest Molding of Expanded Thermoplastic Polyurethane Bead Foams and Their Mechanical Properties," *Chemical Engineering Science* 174 (2017): 337–346.
- 16. J. Jiang, F. Liu, X. Yang, et al., "Evolution of Ordered Structure of TPU in High-Elastic State and Their Influences on the Autoclave Foaming of TPU and Inter-Bead Bonding of Expanded TPU Beads," *Polymer (Guildf)* 228 (2021): 123872, https://doi.org/10.1016/j.polymer.2021.123872.
- 17. J. Jiang, F. Liu, B. Chen, et al., "Microstructure Development of PEBA and Its Impact on Autoclave Foaming Behavior and Inter-Bead Bonding of EPEBA Beads," *Polymer (Guildf)* 256, no. June (2022): 125244, https://doi.org/10.1016/j.polymer.2022.125244.
- 18. J. Kuhnigk, D. Raps, T. Standau, M. Luik, V. Altstädt, and H. Ruckdäschel, "Insights Into the Bead Fusion Mechanism of

- Expanded Polybutylene Terephthalate (E-Pbt)," *Polymers (Basel)* 13, no. 4 (2021): 1–20.
- 19. J. Jiang, L. Wang, F. Tian, Y. Li, and W. Zhai, "Polymer Bead Foams: A Review on Foam Preparation, Molding, and Interbead Bonding Mechanism," *Macromolecules* 3, no. 4 (2023): 782–804.
- 20. J. Gensel, C. Pawelski, and V. Altstädt, "Welding Quality in Polymer Bead Foams: An In Situ SEM Study," *AIP Conference Proceedings* 1914 (2017): 060001.
- 21. J. Kuhnigk, N. Krebs, C. Mielke, T. Standau, D. Pospiech, and H. Ruckdäschel, "Influence of Molecular Weight on the Bead Foaming and Bead Fusion Behavior of Poly(Butylene Terephthalate) (PBT)," *Industrial and Engineering Chemistry Research* 61, no. 49 (2022): 17904–17914.
- 22. M. Dippold, C. Töpfer, and H. Ruckdäschel, "Influence of Dielectric Properties of Polybutylene Terephthalate and Respective Foam Beads on Process Behavior in Radio-Frequency Welding," *Journal of Applied Polymer Science* 141, no. 8 (2024): 1–12, https://doi.org/10.1002/app.54988.
- 23. E. Verdonck, K. Schaap, and L. C. Thomas, "A Discussion of the Principles and Applications of Modulated Temperature DSC (MTDSC)," *International Journal of Pharmaceutics* 192, no. 1 (1999): 3–20.
- 24. Choosing Conditions in Modulated DSC, https://www.tainstruments.com/pdf/literature/TN45.pdf.
- 25. M. Bousmina, H. Qiu, M. Grmela, and J. E. Klemberg-Sapieha, "Diffusion at Polymer/Polymer Interfaces Probed by Rheological Tools," *Macromolecules* 31, no. 23 (1998): 8273–8280.
- 26. R. P. Wool and K. M. O'Connor, "A Theory Crack Healing in Polymers," *Journal of Applied Physics* 52, no. 10 (1981): 5953–5963.
- 27. D. Zouzias, G. De Bruyne, R. Miralbes, and J. Ivens, "Characterization of the Tensile Behavior of Expanded Polystyrene Foam as a Function of Density and Strain Rate," *Advanced Engineering Materials* 22, no. 12 (2020): 1–13, https://doi.org/10.1002/adem.202000794.
- 28. N. Tang, D. Lei, D. Huang, and R. Xiao, "Mechanical Performance of Polystyrene Foam (EPS): Experimental and Numerical Analysis," *Polymer Testing* 73, no. November 2018 (2019): 359–365, https://doi.org/10.1016/j.polymertesting.2018.12.001.